NAIC-ID(RS)T-0492-96

NATIONAL AIR INTELLIGENCE CENTER

SIMULATION AND ANALYSIS OF NONLINEAR EFFECTS OF LASER ATMOSPHERIC PROPAGATION

by

Jiang Shaoen and Sun Jingwen

Approved for public release: distribution unlimited

HUMAN TRANSLATION

NAIC-ID(RS)T-0492-96 8 October 1996

MICROFICHE NR:

SIMULATION AND ANALYSIS OF NONLINEAR EFFECTS OF LASER ATMOSPHERIC PROPAGATION

By: Jiang Shaoen and Sun Jingwen

English pages: 15

Source: Chinese Journal of Lasers; pp. 144-150

Country of origin: China
Translated by: Leo Kanner Associates
F33657-88-D-2188
Requester: NAIC/TATD/Bruce Armstrong
Approved for public release: distribution unlimited.

GRAPHICS DISCLAIMER

All figures, graphics, tables, equations, etc. merged into this translation were extracted from the best quality copy available.

SIMULATION AND ANALYSIS OF NONLINEAR EFFECTS OF LASER ATMOSPHERIC PROPAGATION

*Jiang Shaoen and #Sun Jingwen

*Southwest Institute of Nuclear Physics and Chemistry Science, Chengdu 610003

#Technology Information Center, China Academy of Engineering Physics, Chengdu 610003

ABSTRACT

Simulation of the nonlinear effects of laser atmospheric propagation is reported in this paper. A set of atmospheric hydrodynamic equations and the nonlinear electromagnetic wave equation for interaction with the atmosphere are given. The wave equation describing small-perturbation instability induced by stimulated thermal Rayleigh scattering (STRS)is derived. Also, turbulence is theoretically treated. Based on these equations, we performed a set of 4D programs (TURBLM) to simulate thermal blooming and phase compensation for it, small-perturbation instability, and the interaction of turbulence with thermal blooming. The simulated results are in agreement with theory and experiment.

Key Words: thermal blooming, small-perturbation instability, turbulence.

1. Introduction

The propagation of a high-power laser through the atmosphere is an extremely complex process, even without considering the nonlinear process, which includes a sizable number of factors. Among these, the relatively significant nonlinear effects not involving the internal processes of atmospheric molecules include thermal blooming[1-3], small-perturbation instability resulting from stimulated thermal Rayleigh scattering(STRS)[4-5], as well as interaction between atmospheric turbulence[6] and thermal blooming, etc.

Based on the above-mentioned scenario, a numerical simulation was conducted in this paper, and a 4D program (TURBLM) was written to investigate the foregoing nonlinear processes of high-power laser atmospheric propagation. Apparently, the experiment on laser omnidistance atmospheric propagation can be well simulated if a linear process is introduced into the program without the necessity of making significant modification to its main structure.

2. Thermal Blooming

During high-power laser propagation through the atmosphere, a small portion of energy can be absorbed by the molecules and aerosol in the atmosphere, and the heated air can lead to an increase in gas pressure. As a result, the gas will expand at the speed of sound and the pressure equalizes, giving rise to a decrease in density and lower refractivity, thereby forming a negative lens and causing laser beam divergence.

When there is a laterally-blowing wind, the air density of the descending wind decreases, bringing about lower refractivity of this air and forming a unique crescent beam bending toward the ascending wind; this situation can produce light distortion,

bending and divergence, eventually affecting light beam quality. This kind of effect is called thermal blooming. Thermal blooming can restrict the maximum power in high-power laser propagation through the atmosphere, and this is one of the most critical problems in high-power laser atmospheric propagation.

There are two basic interacting coupled equations in research on thermal blooming, namely, the light wave equation showing the modification of refractivity caused by changes in atmospheric density, and the hydrodynamic equation showing the modification of atmospheric density change resulting from laser heating.

The paraxial wave equation is as follows:

$$2ik\frac{\partial\psi}{\partial z}+\nabla_{\perp}^{2}\psi+k^{2}\left(\frac{n^{2}}{n_{0}^{2}}-1\right)\psi=0 \tag{1}$$

The hydrodynamic equation under constant pressure approximation is as follows:

$$\frac{\partial\rho_{1}}{\partial t}+V\frac{\partial\rho_{1}}{\partial x}=-\frac{\nu-1}{c_{s}^{2}}\alpha I \tag{2}$$

The relation between atmospheric refractivity and density is as follows:

$$n-1=\kappa\rho \tag{3}$$

From Eq. (3),

$$\delta\varepsilon=\frac{n^{2}}{n_{0}^{2}}-1\approx 2(n-n_{0})/n_{0}\approx 2\kappa\rho_{1} \tag{4}$$

where k is the number of waves, ψ is the complex amplitude of optical field, i.e., $E=4\exp[i(kz-\omega t)]$, I is laser light intensity, i.e., $I=(c/4\pi)|\psi|^2$, ρ_0 is standard atmospheric density, ρ_1 is laser induced perturbation density, $\rho=\rho_0+\rho_1$, κ is the Lorentz coefficient, v is wind speed, c_s is speed of sound, $\nu=c_p/cv_o$. Eqs.(1) and (2) constitute a set of coupled equations showing the interaction between laser and atmosphere, which form

the foundation for research on the linear and nonlinear theories of laser atmospheric propagation.

Our simulation of thermal blooming commences from this set of equations, adopting a phase screening method for wave equation (1) as well as the fast Fourier transform (FFT).

Suppose ψ_R is a field at $z=z_R$, then the formal solution at $z_{R+1}=z_R+\Delta z$ is

$$\psi_{n+1} = \exp\left\{\left[\frac{i}{2k}\left(\Delta z\nabla_\perp^2 + k^2\int_{z_n}^{z_{n+1}}\delta\varepsilon dz\right)\right]\cdot\psi_n\right\} \tag{5}$$

Under the binary approximation, the following equation can be formulated:

$$\psi_{n+1} = \exp\left[\left(\frac{i}{4k}\Delta z\nabla_\perp^2\right)\right]\exp\left(\frac{ik}{2}\Delta z\delta\bar{\varepsilon}\right)\exp\left(\frac{i}{4k}\Delta z^2\nabla_\perp\right)\psi_n \tag{6}$$

where

$$\delta\bar{\varepsilon} = \frac{1}{\Delta z}\int_{z_n}^{z_{n+1}}\delta\varepsilon dz$$

and let $\delta\phi_b=(k/2)\Delta z\delta\bar{\varepsilon}$, and let it represent the phase distortion caused by thermal blooming.

It can then be seen from Eq. (6) that owing to the above treatment, the nonlinear term is simplified and acquires a remarkable physical significance. The solution to $z_R \rightarrow z_{R+1}$ can be accomplished in three steps: (1) Free diffraction of the optical field $\Delta z/2$; (2) The nonlinear phase distortion $\delta\phi_b$ introduced due to the modification of atmospheric refractivity is taken into computation; (3) Repeated free diffraction of the optical field $\Delta z/2$.

Two numerical calculation methods are adopted for Eq. (2): one is FFT, while the other is characteristic-type differentiation method.

Based on Eqs. (1) and (2), we edited a 4D program (TURBLM) for numerical simulation. The result of the simulation is in total agreement with the result described in reference 8. In addition, another simulation was also made for thermal blooming compensation, which resulted in a great improvement in light beam quality[8].

3. Small-perturbation Instability

Small-perturbation instability occurs, during stimulated thermal Rayleigh scattering, in atmospheric propagation when no adaptive optics is used. This scattering may be stimulated by sound waves and in this case, it is called stimulated thermal Brillouin scattering (STBS). Also, it may be stimulated by long-time period density variation, referred to as stimulated thermal Rayleigh scattering. The relatively long-time period STRS was our selection. The occurrence of small-perturbation instability has a serious practical effect on high-power laser atmospheric propagation. Atmospheric turbulence and laser noise are stimulation sources for small-perturbation instability. Therefore, for high-quality coherent laser beams in the actual atmosphere, one must suppress the instability or keep the growing small-perturbation still at a low level.

The developmental mechanism of STRS instability is as follows: laser beams with small perturbation are symbolized by superimposition of unperturbed intense beams and weak beams. The intense main laser (pump light) and weak perturbed beam (scattering light) generate interference and constitute interference fringes. The interference fringes can modulate air absorption and heating and modify the refractivity. The intense light can enlarge the refractivity area and transmits energy further to the weak light along the path, thereby intensifying it, i.e., intensifying the perturbation.

There are two methods for numerical computation of the small-perturbation instability. One is to subtract, directly using the thermal blooming program, the optical field of perturbed laser atmospheric propagation from the optical field of unperturbed laser atmospheric propagation. The result of subtraction is the temporal and spatial variation of the perturbation field. This method is simple but its physical concept is not clear. The other method is as follows: when the thermal blooming of the main laser (pump light) is not intense, it is possible to assume that the main laser, not subject to atmospheric effects, undergoes only diffraction and absorption. And the modification of refractivity is basically caused by the interference from the main laser and the perturbation field. The perturbation field is the modification and increase of the scattering light in the atmosphere.

Suppose the overall optical field of the perturbation field is $\psi' = \psi_p + \psi_s$, and the air density variation is $\rho_1' = \rho_{p_1} + \rho_{s_1}$, where the subscripts p and s are quantities related to pump and scattering. ψ' and ρ_1' , respectively, satisfy Eqs. (1) and (2), while ψ_p and ρ_p also satisfy Eqs. (1) and (2). By subtracting the two equations of ψ and ρ, the following can be derived:

$$2ik\frac{\partial \psi_s}{\partial z} + \nabla_\perp^2 \psi_s = -2k^2\kappa(\psi_p\rho_{s_1} + \psi_s\rho_{s_1} + \psi_s\rho_{s_1}) \tag{7}$$

$$\frac{\partial \rho_{s_1}}{\partial t} + v\frac{\partial \rho_{s_1}}{\partial x} = -\frac{\nu - 1}{c_s^2}\alpha(\psi_p\psi_s^* + \psi_p^*\psi_s + \psi_s\psi_s^*) \tag{8}$$

From the above assumption, $\rho_{s_1} \approx 0$, $|\psi_s|^2 \ll |\psi_p\psi_s^*|$, and then the simulation coupled equations of small-perturbation instability are:

$$2ik\frac{\partial \psi_p}{\partial z} + \nabla_\perp^2 \psi_p = 0 \tag{9}$$

$$2ik\frac{\partial \psi_s}{\partial z} + \nabla_\perp^2 \psi_s = 2k^2 \kappa \psi_p \rho_{s_1} \tag{10}$$

$$\frac{\partial \rho_{s_1}}{\partial t} + v\frac{\partial \rho_{s_1}}{\partial x} = -\frac{\nu - 1}{c_s^2}(\psi_p \psi_s^* + \psi_p^* \psi_s) \tag{11}$$

Eq. (9) shows the free diffraction of the pump light in the atmosphere and takes only atmospheric absorption into account. Eq. (10) shows an increasing wave equation, caused by the perturbed optical field under modulation by the pumping light and density. Eq. (11) shows the hydrodynamics equation for the case when interference by the pump light and the perturbation field causes density changes. Eqs. (9)-(11) constitute a set of complete coupled equations specifically for research on STRS induced small-perturbation instability.

Among the simulation parameters that we adopted are the following: the light intensity of the initial pump field is a platform distribution, i.e., I_p=400W/cm^2; laser wavelength is 10.6μm; beam diameter D=50cm; the total power of the pump field is 780kW; the light intensity of initial perturbation is I_s=0.04W/cm^2; the period of the perturbation field is 10cm; absorption coefficient α=0.2x10^{-5}cm^{-1}; and horizontal wind velocity (along the x-direction) v=10m/s.

For the computed perturbative intensity see Fig. 1, where the curves are intensity contours. The given distributive fringes of initial perturbative intensity form a 45^0 angle with the wind direction (along the x-axial direction). It can be seen that the growth direction of small perturbative fringes (i.e., the direction of the contour peaks) gradually approaches the wind direction and eventually becomes parallel to the wind direction. The perturbative field first breaks up and gradually turns in the wind direction before connecting one with another to form fringes along the wind direction. As a result, the growth direction of the perturbative field fringes appears parallel to the wind

direction. Such kind of phenomenon can be interpreted like this: since a small segment of perturbative fringe, blown by the wind, leads to the decrease of air density in the descending wind, while the light is diffracted from a sparse light medium to a dense light medium, this small segment of perturbative fringe approaches to the wind direction. When the propagation distance and time are sufficiently long, the perturbative fringes are parallel to the wind direction.

Additionally, with the growth and change of perturbation in space, its perturbative period generally does not change. In Fig. 1, the number of fringes stays at 5 constantly. But it seems that there are 10 fringes at the transmitting aperture. This is because the sinusoidal distribution is both negative and positive. Actually, there are only 5 fringes. The above two arguments conform to the SABLE experiment (Scaled Atmospheric Blooming Experiment) as described in reference 9. The calculations in the latter are listed in Fig. 2, where the simulation parameters are: number of thermal blooming distortion N_D=220; wind fluctuation $\sigma=\sigma_r/v$=0.45 (σ is variance); number of perturbation modulation is 5; transmitting aperture is 35cm,; wavelength is 2.9μm; power is 10kW; transmission distance z=400m.

Fig. 3 shows the development of perturbative intensity with transmission distance z at two points (a: x=y=0; b: x=20cm, y=0) in horizontal space. The growth and variation of small perturbation can be seen in this figure: the perturbation tends to grow in space when t=0.005s. It grows extremely rapidly because damping is not taken into consideration. For instance, the spreading term of refractivity and random wind are not considered to suppress the growth of small perturbation.

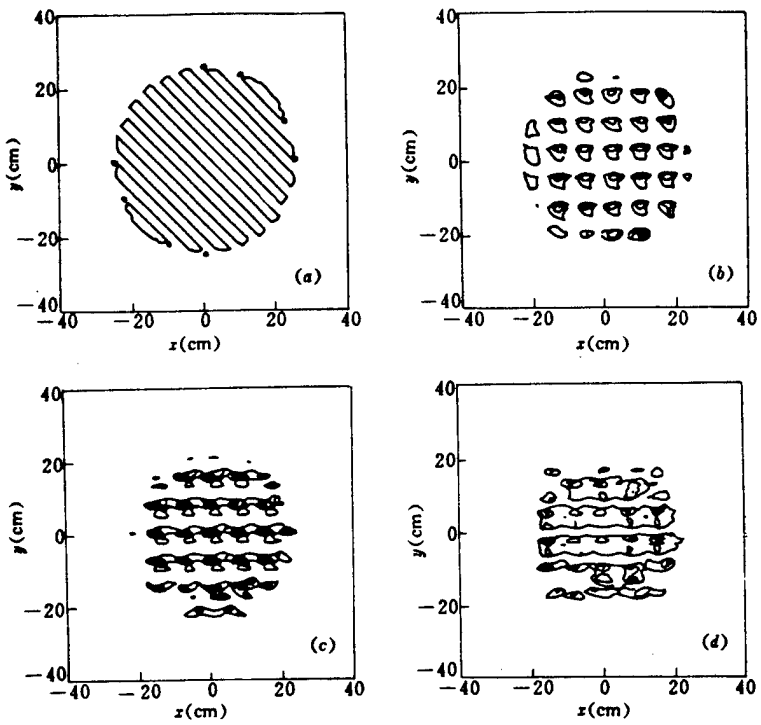

Fig. 1. Perturbative intensity contour along z-direction at t=0.005s

(a) z=0 (b) z=1km (c) z=2km (d) =3km

Fig. 2. Intensity contour on the beacon

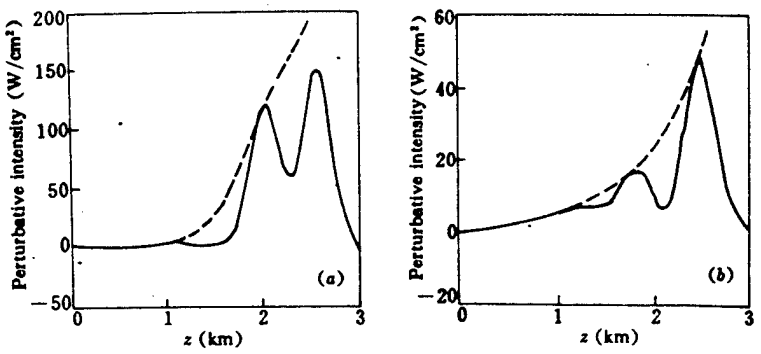

Fig. 3. Perturbative intensity with propagation distance z (a) $x = y = 0$; (b) $x = 20$ cm, $y = 0$

Let us briefly analyze Fig. 3. According to Karr's thermal blooming linear analysis[5], the amplitude of perturbative field intensity changes in time and space variation as follows:

$$I_s(z,t) \propto \exp\left[3\pi\left(\frac{N_\lambda}{4N_f}\right)^{1/3}\right] \tag{12}$$

where $N\lambda=\Gamma_{kzt}/2\pi$ is the number of thermal blooming waves; $\Gamma=(8.25\times10^{-3}\text{cm}^3/\text{J})\alpha I_p$; $N_f = \pi^2 k/2k_p^2 z$ is the perturbation Fresnel number; k_p is the number of perturbative waves. When t=0.005s, by substituting the simulation parameters in Eq. (12),

$$I_s(z,t) \propto \exp[3.3z^{2/3}] \tag{13}$$

where z is in km. From the imaginary line in Fig. 3, it can be calculated that (a) I_S varies as $\exp[4.1z^{2/3}]$, (b) I_s varies as $\exp[2.8z^{2/3}]$. Therefore, we know that the calculations do not closely agree with the analysis results in Eq. (13). This is because Karr's analysis did not consider the effect in the horizontal direction but the horizontal infinite plane wave, while in our calculations, the effect in horizontal direction is taken into account. As a result, the growth of perturbative intensity in horizontal direction is different in both cases. However, our calculations generally conform to linear equation (13). Besides, when the perturbative field grows to a certain

degree, its growth rate will slow down as shown in Fig. 3(a).

4. Effect of Atmospheric Turbulence on Thermal Blooming

The variation process of atmospheric turbulence is a random process, which is to be described with a statistical law. We use the Karman spectrum as its statistical law. Atmospheric turbulence has two kinds of effects on thermal blooming, that is: the turbulent beam expansion can cause changes to intensity distribution and thus directly affect thermal blooming, and turbulence perturbation can affect temperature gradient and cause thermal blooming to change. The computation of the combining action of turbulence and thermal blooming is similar to the computation method without turbulence, but unlike the latter, it is required to add the phase shift $\delta\varphi_t$ introduced by turbulence and the phase shift $\delta\varphi_b$ produced by thermal blooming to form a phase shift caused by interaction between turbulence and thermal blooming $\delta\varphi=\delta\varphi_t+\delta\varphi_b$. The phase distortion created by turbulence is

$$\delta\phi_t = \frac{k}{2}\Delta z\bar{\varepsilon}_t, \qquad \delta\bar{\varepsilon}_t = \frac{1}{\Delta z}\int_{z_n}^{z_{n+1}} \delta\varepsilon_t(x,t,z)\mathrm{d}z$$

where the subscript t represents turbulence as a cause. Thus, the following equation can be derived to calculate $\delta\bar{\varepsilon}_t(x,y)$:

$$\delta\bar{\varepsilon}_t(x,y) = \left(\frac{2\pi}{\Delta z}\right)^{1/2}\int_{-\infty}^{+\infty}\int_{-\infty}^{+\infty} \mathrm{d}k_x\mathrm{d}k_y\exp[i(k_x x + k_y y)]a(k_x,k_y)\Phi_t^{1/2}(k_x,k_y,0) \tag{14}$$

where Φ_z is the Karman spectrum

$$\Phi_t(k) = 0.033C_t^2(k_0^2 + k_x^2 + k_y^2 + k_z^2)^{-11/6} \tag{15}$$

where C_t^2 is the refractivity structure constant, $k_0=2\pi/L_0$, where L_0 is the external scale of turbulence. In this paper, L_0=10m; k_x, k_y, and k_z are components of wave vector; and $\alpha(k_z,k_y)$ is the two-dimensional complex Gaussian random function.

By making the integration of Eq. (14) discrete, the following can be derived:

$$\delta\phi_t(k\Delta x,\ l\Delta y, z) = \frac{2k(\pi\Delta z)^{1/2}\pi^2}{N^2\Delta x\Delta y}(0.033C_n^2)^{1/2}\sum_{m=0}^{N-1}\sum_{n=0}^{N-1}\frac{\exp\left[i\left(\frac{2\pi m}{N}k+\frac{2\pi n}{N}l\right)\right]}{\left[\left(\frac{2\pi}{L_0}\right)^2+\left(\frac{2\pi m}{N\Delta x}\right)^2+\left(\frac{2\pi n}{N\Delta y}\right)^2\right]^{11/12}}$$
$$\cdot\left[a'(m,n)+ia''(m,n)\right] \qquad (16)$$

where $\alpha'(m,n)$ and $\alpha''(m,n)$ are the Gaussian distribution functions with variance 1; N is the number of sample points; Δx and Δy are the intervals between sample points; $k\Delta x$ and $l\Delta y$ are the space location coordinates. Eq. (16) is a working formula for phase distortion caused by atmospheric turbulence.

Using Eq. (16), we computed the interaction between turbulence and thermal blooming with the following simulation parameters: the incident beam is a Gaussian beam; laser wavelength β=10.6μm; power p=80kW; focal length f=6km; beam diameter D=50cm; absorption coefficient $\alpha=0.2\times10^{-5}cm^{-1}$; horizontal wind velocity v=10m/s.

Fig. 4 (a), (b), (c) and (d) respectively are intensity contours on the focal plane when $C_n^2=0$, $10^{-6}m^{-2/3}$, $5\times10^{-16}m^{-2/3}$, $10^{-15}m^{-2/3}$, where $C_n^2=0$ is a pure thermal image without turbulence. It can be seen that turbulence has a rather great effect on thermal blooming. The more intensive the turbulence (the greater the C_n^2), the greater the laser beam expansion and trembling. It can even cause beam to expand, resulting in further decrease of beam quality.

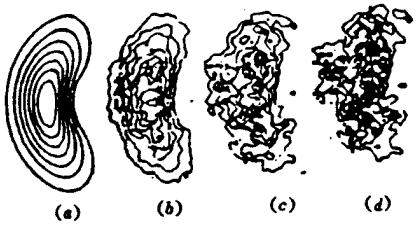

Fig. 4. Intensity contour at focal plane with thermal blooming and turbulence
(a) $C_n^2 = 0$; (b) $C_n^2 = 10^{-16}\,m^{-2/3}$;
(c) $C_n^2 = 5 \times 10^{-16}\,m^{-2/3}$; (d) $C_n^2 = 10^{-15}\,m^{-2/3}$

When there is no turbulence, the number of the thermal blooming distortion is

$$N_c = \frac{I_0 \alpha z^2 dn/dT}{n_0 \rho_0 c_p v a} \tag{17}$$

Based on numerical simulation and experimentation, Gebhardt obtained the following formula:

$$I_{rel} = \frac{1}{1 + 0.0625 N_c^2} \tag{18}$$

where I_{rel} is the ratio between the intensity with thermal blooming and intensity under linear absorption, which is a parameter indicating the beam quality; when $N_c=0$, $I_{rel}=1$, i.e., the beam is not distorted. By substituting simulation parameters in Eq. (17), $N_c=23$, and $I_{rel}=0.03$ can be obtained. Based on Fig. 4(a), $I_{rel}=0.035$ can be computed, which is close to the calculated value from Eq. (18). For images with turbulence, $I_{rel}=0.028$, 0.015, and 0.012 can be calculated, respectively, from Fig. 4(b), (c), and (d). It is known therefore that turbulence has a small effect on thermal blooming when $C_n^2 = 10^{-16} m^{-2/3}$, but it has a strong effect on thermal blooming when $C_n^2 \geq 5 \times 10^{-15} m^{-2/3}$.

5. Conclusions and Discussion

The following conclusions can be reached based on the above analysis and calculations in this paper:

(1) There is small-perturbation instability in laser atmospheric propagation, which has an unfavorable effect on the main laser;

(2) Small-scale growing fringes approach toward the wind direction, and the perturbation period basically remains unchanged;

(3) The strength of atmospheric turbulence has different effects on laser atmospheric propagation.

This paper mainly discussed thermal blooming, STRS induced instability and the interaction between thermal blooming and turbulence. It is noteworthy that there is still small-perturbation instability caused by the stimulated thermal Brillouin scattering (STBS) in high-power laser atmospheric propagation. The major difference between STBS and STRS lies in that there is frequency shift between scattering light and incident light in STBS ($k\neq 0$, $\hat{\omega}\neq 0$). Since STBS takes place in the transient process of thermal blooming and the transient process is only 3-5 times the hydrodynamics time t_H($t_H \approx D/C_s$; D is beam diameter, C_s is the speed of sound), STRS has a small effect on the continuous laser beams. However, its effect on pulsed laser propagation cannot be neglected.

This paper was received for editing on March 4, 1993. The edited paper was received on June 27, 1995.

REFERENCES

1 D. C. Smith. High-power laser propagation: thermal blooming. *Proc. IEEE*, 1977, **65**: 1679～1714

2 J. L. Walsh, P. B. Ulrich. Thermal blooming in the atmosphere, in (Laser Beam Propagation in the Atmosphere). J. W. Strobehn ed., New York: Springer-Verlag, 1978

3 F. G. Gebhardt. Twenty-five years of thermal blooming: an overview. *Proc. SPIE*, 1990, **1221**: 2～25

4 T. J. Karr. Perturbation growth by thermal blooming in turbulence. *J. Opt. Soc. Am. B*, 1990, **7**: 1103～1124

5 T. J. Karr. Instabities of atmospheric laser propagation. *Proc. SPIE*, 1990, **1221**: 26～57

6 F. G. Gebhardt, D. C. Smith, R. G. Buser *et al.*. Turbulence effects on thermal blooming. *Appl. Opt.*, 1973, **12**: 1794～1805

7 J. A. Fleck, J. R. Morris, M. J. Feit. Time dependent propagation of high energy laser beams through the atmosphere. *Appl. Phys. Lett.*, 1976, **10**: 129～160

8 J. Wallace, J. Q. Lilly. Thermal blooming of repetitively pulse laser beams. *J. Opt. Soc. Am.*, 1974, **64**: 1651～1655